Please cite this article in press as: Bonath et al., Neural Basis of the Ventriloquist Illusion, Current Biology (2007), doi:10.1016/j.cub.2007.08.050

Current Biology *17*, 1–7, October 9, 2007 ©2007 Elsevier Ltd All rights reserved DOI 10.1016/j.cub.2007.08.050

Report

Neural Basis of the Ventriloquist Illusion

Bjoern Bonath,[1,2,5] Toemme Noesselt,[2,3,5,*] Antigona Martinez,[1,4] Jyoti Mishra,[1] Kati Schwiecker,[2] Hans-Jochen Heinze,[2] and Steven A. Hillyard[1]
[1]Department of Neurosciences
University of California, San Diego
9500 Gilman Drive
La Jolla, California 92093-0608
[2]Department of Neurology II
Otto-von-Guericke-University
Leipziger Str. 44
39120 Magdeburg
Germany
[3]Institute for Cognitive Neurosciences
University College London
17 Queen Square
London WC1N 3AR
United Kingdom
[4]Nathan S. Kline Institute for Psychiatric Research
140 Old Orangeburg Road
Orangeburg, New York 10962

Summary

The ventriloquist creates the illusion that his or her voice emerges from the visibly moving mouth of the puppet [1]. This well-known illusion exemplifies a basic principle of how auditory and visual information is integrated in the brain to form a unified multimodal percept. When auditory and visual stimuli occur simultaneously at different locations, the more spatially precise visual information dominates the perceived location of the multimodal event. Previous studies have examined neural interactions between spatially disparate auditory and visual stimuli [2–5], but none has found evidence for a visual influence on the auditory cortex that could be directly linked to the illusion of a shifted auditory percept. Here we utilized event-related brain potentials combined with event-related functional magnetic resonance imaging to demonstrate on a trial-by-trial basis that a precisely timed biasing of the left-right balance of auditory cortex activity by the discrepant visual input underlies the ventriloquist illusion. This cortical biasing may reflect a fundamental mechanism for integrating the auditory and visual components of environmental events, which ensures that the sounds are adaptively localized to the more reliable position provided by the visual input.

Results and Discussion

In the present study, we investigated the neural basis of the ventriloquist illusion [1], that is, the mislocalization of sounds toward the position of co-occurring visual stimuli. Twenty-two subjects were instructed to report the perceived location of brief auditory stimuli (10 ms tone pip) that were presented from nonvisible free-field speakers situated at left (A_L), right (A_R), and center (A_C) locations (Figure 1A). These tones could occur either by themselves or in combination with simultaneous flashes from LEDs situated at the left (V_L) and right (V_R) of the display. These five unimodal stimuli and four bimodal combinations (A_CV_L, A_CV_R, A_RV_L, A_LV_R) were presented in random order at intervals of 1.2–1.8 s. Subjects were told to ignore the visual stimuli and to simply report the position of each sound as left, right, or center. The subjects' behavioral responses showed that their perception of sound location was shifted toward the position of a concurrent visual stimulus (see Table 1).

To study the neural basis of these behavioral ventriloquist effects, event-related potentials (ERPs) were recorded to each type of stimulus during task performance. Multimodal interactions were revealed in the difference waveforms formed by subtracting the sum of the ERPs to the constituent unimodal stimuli from the ERP to their bimodal combination [6–9]. These subtractions also included blank or no-stimulus events (ERPs triggered at a time when no stimulus was presented) in order to cancel out any prestimulus activity common to all stimuli, which would be added once but subtracted twice in the difference waveforms [3, 10–12]. Thus, for example, the multimodal interaction between a central sound and a flash to the left would be revealed in the ERP difference waveform $[(A_CV_L + \text{blank}) - (A_C + V_L)]$.

The multimodal difference ERPs associated with the central sound/lateral flash combinations (i.e., A_CV_L and A_CV_R) were calculated separately for trials where the auditory percept was shifted toward the location of the flash (illusion trials; Figure 1B) and trials where the sound was correctly localized to the center (no-illusion trials; Figure 1C). These difference waveforms included two prominent interaction components, a positivity peaking at around 180 ms (P180) and a negativity peaking at around 260 ms (N260). Whereas the P180 was bilaterally symmetrical over the scalp for all conditions, the N260 was symmetrical for no-illusion trials but was larger over the hemisphere contralateral to the side of the visual stimulus (and hence contralateral to the side of the shifted auditory percept) for illusion trials. This asymmetry was reflected in a significant illusion (present-absent) by hemisphere (contralateral-ipsilateral to flash) interaction for the N260 amplitude ($F(1,21) = 10.2$, $p < .004$); post hoc tests showed that N260 over the hemisphere ipsilateral to the side of the visual stimulus was reduced relative to the contralateral amplitude on illusion trials ($p < .01$) and was reduced relative to the amplitude for the no-illusion trials over both hemispheres ($p < .01$ for both). There was no significant hemispheric asymmetry on the no-illusion trials (contra-ipsi hemisphere effect, n.s.). A similar illusion-related asymmetry of N260 in the interaction difference waveforms

*Correspondence: toemme@med.ovgu.de
[5]These authors contributed equally to this work.

Please cite this article in press as: Bonath et al., Neural Basis of the Ventriloquist Illusion, Current Biology (2007), doi:10.1016/j.cub.2007.08.050

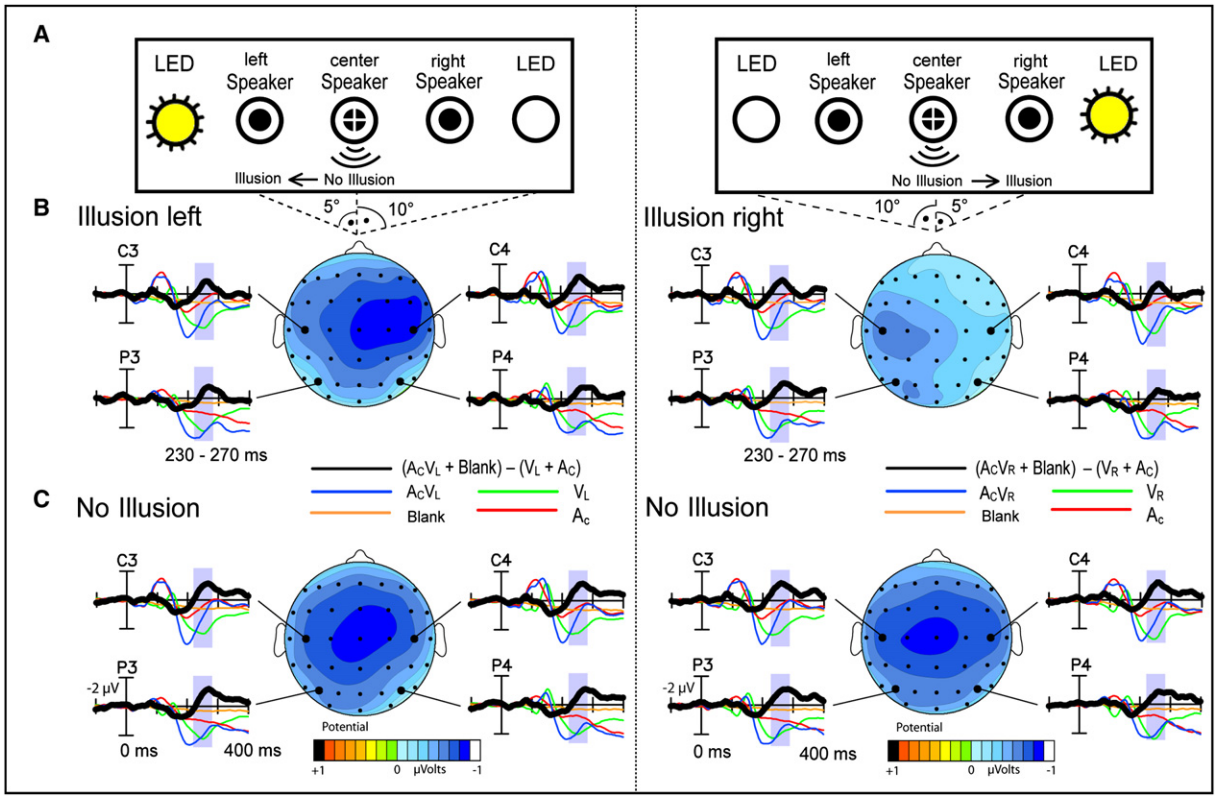

Figure 1. Experimental Stimuli and Grand Averaged ERPs Associated with Ventriloquist Illusion

(A) Tones were presented from left, center, or right speakers, either alone or in combination with flashes from LEDs on the right or left side. Left: stimulus combination of central tone (A_C) + left flash (V_L). Right: central tone (A_C) + right flash (V_R) combination.

(B) Grand averaged ERP waveforms to auditory (red), visual (green), blank (orange), and audiovisual (blue) stimuli, together with the multimodal difference waves [(AV + blank) − (A + V)] (thick black) recorded from central (C3, C4) and parietal (P3, P4) electrodes on trials where the ventriloquist illusion was present (i.e., subjects perceived the sound as coming from the speaker on the same side as the flash). Topographical voltage maps are of the N260 component measured as mean amplitude over 230–270 ms (shaded areas) in the multimodal difference waves. Note larger amplitude contralateral to the side of flash and perceived sound.

(C) Grand average ERPs and topographical voltage distributions of N260 on trials where the ventriloquist illusion was absent (i.e., subjects correctly reported sound location at the center). Note bilaterally symmetrical voltage distributions of N260.

was found for trials with the A_RV_L and A_LV_R stimuli, on which the perceived sound locations were shifted significantly to the center when the flash occurred on the opposite side. Again, the N260 in the difference waveform was larger over the hemisphere contralateral to the visual stimulus relative to the ipsilateral hemisphere (illusion × hemisphere interaction: $F(1,21) = 10.8$, $p < .003$).

To identify the brain regions where this illusion-related ERP asymmetry was generated, the neural sources of the N260 were estimated by dipole modeling (BESA

Table 1. Behavioral Data Showing Ventriloquist Illusion in the ERP Experiment

Stimulus	Respond Left %	SEM	Respond Center %	SEM	Respond Right %	SEM
A_L	69.0[a]	3.3	27.2	2.8	3.0	0.8
A_C	11.6	1.6	69.3[a]	2.8	18.2	2.6
A_R	2.3	0.7	20.7	1.8	75.5[a]	2.2
A_CV_L	32.4[b]	4.9	57.2[a]	4.4	8.8	1.5
A_CV_R	6.1	1.2	55.8[a]	4.5	36.3[c]	4.9
A_LV_R	51.7[a]	4.7	34.8[d]	3.0	12.3[e]	4.2
A_RV_L	12.6[f]	4.2	28.1[g]	2.6	58.1[a]	4.3

Percentage of trials on which subjects judged the sound location to be at the left ($_L$), center ($_C$), or right ($_R$) for each of the unitary auditory (A) stimuli and for the bimodal auditory-visual (AV) combinations. Significance levels of vision-induced shifts in auditory localization are indicated in the footnotes. Corresponding behavioral data from the fMRI experiment are shown in Table S1.

[a] Correct response percentage.

[b] Left responses: A_CV_L versus A_C ($t = -5.1$, $p < .001$).

[c] Right responses: A_CV_R versus A_C ($t = -5.1$, $p < .001$).

[d] Center responses: A_LV_R versus A_L ($t = -3.3$, $p < .003$).

[e] Right responses: A_L versus A_LV_R ($t = -2.6$, $p < .016$).

[f] Left responses: A_R versus A_RV_L ($t = -2.7$, $p < .013$).

[g] Center responses: A_RV_L versus A_R ($t = -3.8$, $p < .001$).

Please cite this article in press as: Bonath et al., Neural Basis of the Ventriloquist Illusion, Current Biology (2007), doi:10.1016/j.cub.2007.08.050

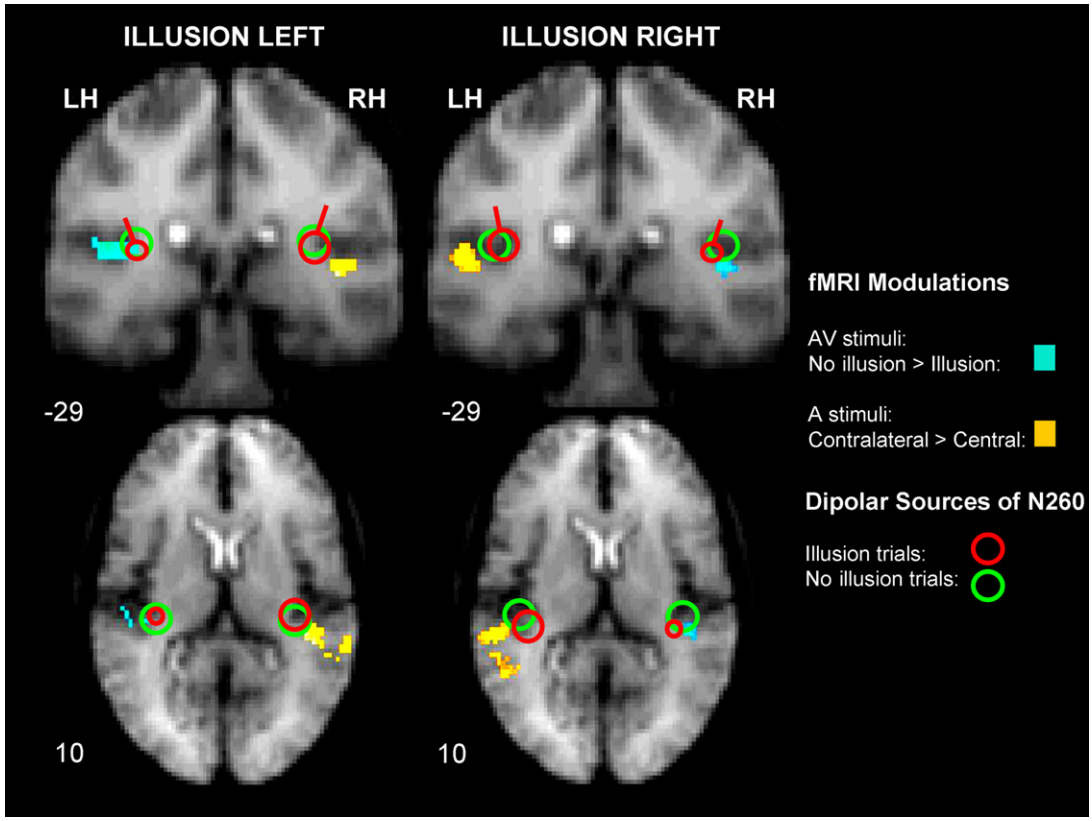

Figure 2. Dipolar Sources of ERPs and fMRI Activations Associated with the Ventriloquist Illusion, Superimposed on the Overall Averaged Brain of the fMRI Group Aligned in Talairach Coordinates

Dipoles were fit by BESA to the topographical voltage distributions of the N260 component shown in Figure 1. Dipoles on brain sections at left were fit to the N260 in the multimodal difference waves [(A_CV_L + blank) – (A_C + V_L)] on trials when the illusion was present (red dipoles) and absent (green dipoles). These dipoles accounted for 92.4% of the scalp voltage variance. Dipoles on sections at right were similarly fit to the N260 in the difference waves [(A_CV_R + blank) – (A_C + V_R)] and accounted for 90.3% of the scalp voltage variance. Note smaller size (i.e., reduced strength) of red dipole ipsilateral to side of illusory sound perception, reflecting the contralateral distribution of the N260 on illusion trials. fMRI modulations in blue show regions where activation was reduced ipsilaterally on illusion versus non-illusion trials for the A_CV_L stimuli (left sections) and the A_CV_R stimuli (right sections). fMRI modulations in yellow show regions where the activation was greater for contralateral sounds than for central sounds (i.e., for left column, $A_L > A_C$; for right column, $A_R > A_C$). Talairach coordinates of each section given below.

algorithm) and compared with the sites of illusion-related activation obtained in a parallel experiment by fMRI. The fMRI experiment (with 12 different subjects) was identical in design to the ERP experiment except that the stimulus parameters and interstimulus intervals were modified to conform with the constraints of the scanning environment (see Experimental Procedures). As shown in Figure 2, the N260 sources were modeled by a bilateral pair of dipoles located in the medial aspect of the planum temporale within the sylvian fissure for both the illusion and no-illusion trials. As expected from the scalp distribution data, the dipole strength of the N260 was reduced in the hemisphere ipsilateral to the perceived sound position in accordance with its lateralized scalp topography.

The calculated position of the N260 dipoles corresponded well with the location of the lateralized BOLD signal in the planum temporale seen in the fMRI experiment. Specifically, in contrasts between illusion and no-illusion trials for the A_CV_L and A_CV_R stimuli, the fMRI showed a reduced BOLD signal on illusion trials in the planum temporale ipsilateral to the side of perceived sound location (Figure 2, blue voxels; see Table 2 for coordinates). Also shown in Figure 2 are lateralized BOLD activations produced by left and right unimodal auditory stimuli relative to central stimuli (yellow voxels). As was the case for the illusion-producing bimodal trials, greater activation was seen in the auditory cortex of the planum temporale contralateral to the unimodal sounds (Table 2), which were correctly localized to the same spatial position as the ventriloquized sounds on bimodal illusion trials.

These converging ERP and fMRI results demonstrate that spatially discrepant auditory and visual stimuli provoke a lateralized neural interaction in auditory cortex in the planum temporale (PT), but only on trials where the ventriloquism illusion of shifted sound perception toward the side of the flash is present. Both the ERP and the BOLD response showed a reduced amplitude in the PT of the hemisphere ipsilateral to the side of the visual stimulus, resulting in a relatively enlarged response in the PT contralateral to the side of the shifted auditory percept. Such an asymmetrical neural response was also produced in auditory cortex by sounds that were actually presented to one side, because of the well-known contralateral preponderance of the human

Please cite this article in press as: Bonath et al., Neural Basis of the Ventriloquist Illusion, Current Biology (2007), doi:10.1016/j.cub.2007.08.050

Table 2. Talairach Coordinates and Significance Levels of Lateralized fMRI Activations in Planum Temporale Contrasting No-Illusion versus Illusion Trials for Bimodal Stimuli and Contrasting Lateral versus Central Auditory Stimulus Presentations

T	p	x	y	z	Anatomical Region
Illusion-Related Activations[a]					
A_CV_L Trials: Illusion < No Illusion in Left Hemisphere					
3.22	0.001	−44	−32	13	L planum temporale
A_CV_R Trials: Illusion < No Illusion in Right Hemisphere					
3.23	0.001	44	−29	11	R planum temporale
Unimodal Auditory Activations[b]					
$A_R > A_C$ in Left Hemisphere					
3.14	0.001	−55	−34	15	L planum temporale
$A_L > A_C$ in Right Hemisphere					
2.37	0.01	45	−32	13	R planum temporale

Additional cortical activations for these contrasts are shown in Table S2.

[a] For the illusion versus no-illusion contrasts, effects were thresholded at $p < 0.05$ after an omnibus F test at 0.00001 [46]. Only clusters with more than 10 contiguous voxels are reported.

[b] For the A_R versus A_C and A_L versus A_C comparisons, effects were thresholded at $p < 0.05$ within areas that showed a significant auditory > visual modulation ($p < 0.001$) [15].

auditory pathways [13–15]. Thus, subjects reported the illusory shift of the sound toward the flash location only on trials where the bimodal auditory/visual stimulus elicited a contralateral-dominant pattern, as would be elicited if the sound were actually at the shifted position.

The ventriloquist illusion provides a classic example of how sensory inputs from the different modalities are integrated in the brain to achieve unified and coherent internal representations of environmental events [1]. The neural mechanisms that subserve multimodal integration have been studied in animals by neurophysiological techniques [8, 16, 17] and in humans by means of neuroimaging [18, 19] and electrophysiological recordings [4, 7, 11, 20]. Interactions between sensory inputs in different modalities have been observed in multiple brain regions including multimodal cortical areas [16, 19, 21, 22] as well as in cortical regions traditionally considered unimodal [16, 17, 19, 23–25].

An important aspect of multimodal integration is the dominance of visual input for specifying the perceived location of an external event [26]. Thus, when concurrent auditory and visual inputs are presented from different locations, the perceived location of the sound is shifted toward the location of the visual stimulus, a phenomenon that has come to be known as the ventriloquist illusion. Although many behavioral experiments have demonstrated the robustness of the ventriloquist illusion under a wide range of conditions [1, 27], only a few studies have examined patterns of neural interaction in the human brain between auditory and visual stimuli presented to spatially disparate locations and thus likely to induce the illusion [2–5]. None of these studies, however, obtained evidence for a visual influence on the auditory cortex response to sound that could be directly linked on a trial-by-trial basis to the ventriloquist illusion of a shifted auditory percept.

The present ERP recordings showed that the presence of the ventriloquist illusion was associated with laterally biased cortical activity between 230 and 270 ms (the N260 component) that was revealed in auditory-visual interaction waveforms. This N260 component elicited on the illusion trials was colocalized with a lateralized BOLD response situated in the posterior/medial region of the auditory cortex in the planum temporale (PT). Studies in both human and nonhuman primates have shown this caudal/medial region receives multimodal inputs and that both excitatory and inhibitory influences of visual input on auditory processing can occur [28–31]. Human neuroimaging studies further indicate that this same area is involved in the analysis of auditory spatial relations [32, 33] and it has been proposed that activation of the posteriomedial PT is a neural correlate of acoustic space [34]. The present results are in accord with these findings and suggest further that asymmetrical activation of the PT forms the neural basis of the lateral shift in sound perception produced by the spatially discrepant visual stimulus.

Previous studies of auditory-visual interaction have observed late negative components in ERP difference waves that closely resemble the present N260 component [2, 4, 11, 12], but the present study is the first to our knowledge to demonstrate its relationship to auditory spatial perception. The relatively long latency of the illusion-related N260 asymmetry suggests that the visual influence on auditory spatial processing is mediated by pathways from visual cortex to multimodal association areas and thence to the auditory cortex. Although further studies are needed to trace the exact pathways involved, recent human ERP evidence is consistent with a long-latency visual influence on auditory spatial processing. Recordings of visual ERPs have shown that retinotopically organized activity is elicited in extrastriate occipital cortex in the time frame 80–120 ms [35] and that location-specific auditory-visual interactions appear first in occipito-temporal and parietal regions at 140–190 ms and then in superior temporal cortex beginning at around 200 ms [3–4]. Neural interactions associated with auditory space perception were also observed after 200 ms in superior temporal and temporal-parietal areas [36]. Thus, whereas auditory location is initially encoded at very early levels of the auditory pathways (even in the brainstem), the perception of auditory space and its modification by concurrent visual input may well depend on longer latency neural interactions (see Supplemental Results and Discussion available online for further discussion of convergent results from studies in macaques).

Another possibility to consider is that the late N260 asymmetry that we observed is a consequence of the reflexive orienting of attention to the illusory sound position, which results in enhanced processing of the sound in auditory cortex [2]. Whereas such an attention mechanism might conceivably contribute to the ventriloquist illusion, our failure to observe any differential BOLD response on illusion trials in the anterior cingulate or posterior parietal cortex—classical markers for an engagement of the attentional network [37, 38]—suggests that attentional orienting does not play a substantial role in the present experiment. Recent behavioral findings further indicate that the influence of visual attention on the ventriloquist illusion is small at best [39, 40].

Please cite this article in press as: Bonath et al., Neural Basis of the Ventriloquist Illusion, Current Biology (2007), doi:10.1016/j.cub.2007.08.050

It has been proposed that response bias may influence behavioral measures of the ventriloquist illusion, with subjects tending to direct their responses toward the position of the visual event regardless of their auditory perception [41]. Several lines of investigation, however, have found that the illusion persists under condition where response bias was ruled out or made highly unlikely ([42, 43]; see [1] for review). The behavioral results from the present ERP experiment (Table 1) are also at odds with a simple response bias effect that favors responding to the specific location of the visual event. On the A_LV_R and A_RV_L trials, there was a significant increase in subject reports of a perceived center location (relative to A_L and A_R trials). Such a result would be expected if the flashes produced a true shift in perceived sound location. Moreover, the present finding of lateralized neural activity in auditory cortex of the PT is in line with previous proposals based on behavioral evidence that the ventriloquist illusion is a true perceptual phenomenon engendered within modality-specific cortex rather than being a consequence of postperceptual response bias or competition [1]. Nevertheless, further studies may be needed to quantify any possible influence of a response bias effect on the neural measures reported here.

In sum, the observed shift in perceived sound location toward the position of a concurrent visual stimulus (ventriloquist illusion) was found to be linked on a trial-by-trial basis with a lateralized pattern of neural activity in the auditory cortex of the planum temporale. The effect of the visual stimulus on illusion-present trials was to produce a relatively greater activation in auditory cortex contralateral to the shifted sound position, similar to that produced by an actual sound at that position. Combined ERP recordings and fMRI showed that this asymmetrical activity occurred in the time range 230–270 ms after stimulus onset and was localized to a region of the planum temporale that has been implicated in the encoding of auditory space [32]. This cortical biasing may represent a neural code for the shift in perceived spatial position of sounds that occur concurrently with visual events at discrepant locations.

Experimental Procedures

Subjects

Twenty-two right-handed, neurologically normal volunteers (10 women, mean age 24 years) were paid to participate in the ERP study after signing written informed consent. An additional 12 normal subjects (5 female, mean age 24 years) participated in the fMRI experiment under identical task and stimuli conditions. All subjects had normal or corrected-to-normal vision and normal hearing.

Stimuli and Apparatus

Subjects sat in a dimly lit, sound-attenuated chamber and fixated a central cross located 130 cm away and measuring 0.4° of visual angle. Auditory stimuli were brief (10 ms) 2 KHz tones with an amplitude of 76 dB. The tones were delivered from one of three loudspeakers, located centrally at fixation (A_C) or 5° to the left (A_L) and right (A_R) of fixation. The speaker array was covered with black linen to avoid visual information regarding speaker position. Brief (10 ms) visual stimuli were delivered from white LEDs (luminance = 140 cd/m^2) located 10° to the right (V_R) and left (V_L) of fixation.

Design

Each subject took part in 15 runs consisting of a total of 3000 trials (20 trials per condition/run). Subjects were initially trained on a single run with only sounds presented at the three locations and on an additional run that contained all stimulus types. Flashes and tones could either occur simultaneously (AV stimuli) or as single unimodal events (A and V stimuli). A total of nine different stimulus conditions (V_L, V_R, A_L, A_C, A_R, A_CV_L, A_CV_R, A_RV_L, A_LV_R), were presented in random order with SOAs varying between 1200 and 1800 ms. To compensate for slow anticipatory brain potentials, an additional "blank" condition was included without any stimulation [11].

Subjects performed a sound localization task and were explicitly instructed to ignore the visual stimuli. Responses were made on a keyboard with one of three fingers to indicate the location of the perceived tone (central, left, or right). Half of the subjects responded with the right hand, and the remaining half responded with the left hand.

ERP Recording and Analysis

The electroencephalogram (EEG) was recorded from 62 electrode sites with a modified 10-10 system montage [4]. All scalp channels were referenced to an electrode at the right mastoid but were algebraically re-referenced offline to the average of the left and right mastoids. Horizontal eye movements were monitored bipolarly via electrodes at the left and right outer canthi. Blinks and vertical eye movements were recorded with an electrode below the left eye, also referenced to the right mastoid. The EEG was digitized at 250 Hz with an amplifier bandpass of 0.01 to 80 Hz (half amplitude low- and high-frequency cutoffs, respectively). Computerized artifact rejection was performed prior to signal averaging in order to discard epochs in which deviations in eye position, blinks, or amplifier blocking occurred.

ERPs elicited by each stimulus condition were averaged in 500 ms epochs with a 100 ms prestimulus baseline. These averages were digitally low-pass filtered with a Gaussian finite impulse function (3 dB attenuation at 46 Hz) to remove high-frequency noise produced by muscle movements and external electrical sources.

Cross-modal interactions were revealed by subtracting the summed ERPs elicited by the unimodal A and V stimuli from the summed ERPs elicited by the bimodal AV and blank stimuli [i.e., $(A_CV_R + \text{blank}) - (V_R + A_C)$ and $(A_CV_L + \text{blank}) - (V_L + A_C)$]. These crossmodal difference waves were calculated separately for "illusion trials" on which the auditory percept was localized to the same location as the simultaneous visual event and "no-illusion trials" in which the location of the sound was correctly reported.

Statistical Analysis

Crossmodal interaction effects were calculated by a three-way repeated-measures analysis of variance (ANOVA) with factors of perception (illusion versus no illusion), visual stimulus location (V_L versus V_R), and hemisphere (left versus right). Difference wave components were quantified as mean amplitudes within specific latency windows centered around the peak of each component with respect to the mean voltage of a 100 ms prestimulus baseline. Each of these components was measured as the mean voltage over two centroparietal electrode clusters (nine electrodes per hemisphere) where its amplitude was maximal.

Dipole Modeling

The locations of the dipolar sources of the illusion-related N260 ERP component were estimated with the Brain Electrical Source Analysis software (BESA version 5.0). A pair of dipoles constrained to be symmetrical in location but allowed to vary freely in orientation was fit to the N260 in the grand-averaged crossmodal difference waves over the latency range used for statistical testing (230–270 ms). In order to estimate the positions of the dipoles with respect to brain anatomy and fMRI activations, the dipole coordinates were transformed into the standardized coordinate system of Talairach and Tournoux [44].

fMRI Methods

During silent interscan periods (see below for fMRI protocol), auditory stimuli (0.5 kHz tones, 80 dB, 10 ms duration) were emitted from piezo-electric speakers above the subject's head inside the scanner at either 0° or ±13° eccentricity. Visual stimuli consisted of 10 ms light flashes emitted from a bundle of fiber-optic cables attached to 9 white LEDs outside the scanning room (size, 3.5°;

Please cite this article in press as: Bonath et al., Neural Basis of the Ventriloquist Illusion, Current Biology (2007), doi:10.1016/j.cub.2007.08.050

luminance, 130 cd/m^2) positioned 25° to the left and right of a central fixation point. The slightly larger stimulus eccentricity of the fMRI experiment was necessary because of the restricted space inside the scanner bore. Eye movements were monitored throughout scanning by a custom-made infrared eye-tracking device [45].

fMRI data were acquired on a whole-body Siemens 3 T Trio-scanner (Siemens, Erlangen, Germany) with an 8-channel phased-array head coil. Volumes (125 volumes per run, FOV: 200 × 200 mm, TR/TE/flip angle = 2000 ms/30 ms/80°, intervolume pause 2000 ms, 32 slices, spatial resolution 3.5 × 3.5 × 4 mm) from 6 runs were acquired for each subject (mean ISI: 3000 ms [range: 2100–6400 ms, poisson distributed], 16 trials per condition per run, 8.3 min run length). To allow for accurate sound localization, stimuli were presented during the silent periods between two scans. The first four volumes of each run were discarded and the remaining volumes were slice-time-acquisition corrected, realigned, normalized, and smoothed (6 mm FWHM) by SPM2 (Wellcome Department, UCL, London, UK.). After preprocessing, all trial types were modeled with the canonical hemodynamic response function (hrf) for each subject. For the second-level group analysis, a repeated-measures ANOVA was computed by SPM2.

Supplemental Data

Two tables and Results and Discussion are available at http://www.current-biology.com/cgi/content/full/17/19/■■■/DC1/.

Acknowledgments

This research was supported by grants from the Deutsche Forschungsgemeinschaft (SFB-TR31/TPA8) and from the National Eye Institute (EY 016984-32).

Received: June 19, 2007
Revised: August 22, 2007
Accepted: August 22, 2007
Published online: September 20, 2007

References

1. Vroomen, J., and De Gelder, B. (2004). Perceptual effects of cross-modal stimulation: ventriloquism and the freezing phenomenon. In The Handbook of Multisensory Processes, G.A. Calvert, C. Spence, and B.E. Stein, eds. (Cambridge, MA: The MIT Press), pp. 141–150.
2. Busse, L., Roberts, K.C., Crist, R.E., Weissman, D.H., and Woldorff, M.G. (2005). The spread of attention across modalities and space in a multisensory object. Proc. Natl. Acad. Sci. USA *102*, 18751–18756.
3. Gondan, M., Niederhaus, B., Rosler, F., and Roder, B. (2005). Multisensory processing in the redundant-target effect: a behavioral and event-related potential study. Percept. Psychophys. *67*, 713–726.
4. Teder-Salejarvi, W.A., Di Russo, F., McDonald, J.J., and Hillyard, S.A. (2005). Effects of spatial congruity on audio-visual multimodal integration. J. Cogn. Neurosci. *17*, 1396–1409.
5. Bischoff, M., Walter, B., Blecker, C.R., Morgen, K., Vaitl, D., and Sammer, G. (2007). Utilizing the ventriloquism-effect to investigate audio-visual binding. Neuropsychologia *45*, 578–586.
6. Molholm, S., Ritter, W., Murray, M.M., Javitt, D.C., Schroeder, C.E., and Foxe, J.J. (2002). Multisensory auditory-visual interactions during early sensory processing in humans: a high-density electrical mapping study. Brain Res. Cogn. Brain Res. *14*, 115–128.
7. Fort, A., Delpuech, C., Pernier, J., and Giard, M.H. (2002). Early auditory-visual interactions in human cortex during nonredundant target identification. Brain Res. Cogn. Brain Res. *14*, 20–30.
8. Stein, B., and Meredith, M. (1993). The Merging of the Senses (Cambridge, MA: The MIT Press).
9. Murray, M.M., Molholm, S., Michel, C.M., Heslenfeld, D.J., Ritter, W., Javitt, D.C., Schroeder, C.E., and Foxe, J.J. (2005). Grabbing your ear: rapid auditory-somatosensory multisensory interactions in low-level sensory cortices are not constrained by stimulus alignment. Cereb. Cortex *15*, 963–974.
10. Teder-Sälejärvi, W.A., McDonald, J.J., Di Russo, F., and Hillyard, S.A. (2002). An analysis of audio-visual crossmodal integration by means of event-related potential (ERP) recordings. Cogn. Brain Res. *14*, 106–114.
11. Talsma, D., and Woldorff, M.G. (2005). Selective attention and multisensory integration: multiple phases of effects on the evoked brain activity. J. Cogn. Neurosci. *17*, 1098–1114.
12. Mishra, J., Martinez, A., Sejnowski, T.J., and Hillyard, S.A. (2007). Early cross-modal interactions in auditory and visual cortex underlie a sound-induced visual illusion. J. Neurosci. *27*, 4120–4131.
13. Pavani, F., Macaluso, E., Warren, J.D., Driver, J., and Griffiths, T.D. (2002). A common cortical substrate activated by horizontal and vertical sound movement in the human brain. Curr. Biol. *12*, 1584–1590.
14. Recanzone, G.H. (2000). Spatial processing in the auditory cortex of the macaque monkey. Proc. Natl. Acad. Sci. USA *97*, 11829–11835.
15. Krumbholz, K., Schonwiesner, M., Rubsamen, R., Zilles, K., Fink, G.R., and von Cramon, D.Y. (2005). Hierarchical processing of sound location and motion in the human brainstem and planum temporale. Eur. J. Neurosci. *21*, 230–238.
16. Kaas, J.H., and Collins, C.E. (2004). The resurrection of multisensory cortex in primates. In The Handbook of Multisensory Processes, G.A. Calvert, C. Spence, and B.E. Stein, eds. (Cambridge, MA: Bradford), pp. 285–294.
17. Budinger, E., Heil, P., Hess, A., and Scheich, H. (2006). Multisensory processing via early cortical stages: connections of the primary auditory cortical field with other sensory systems. Neuroscience *143*, 1065–1083.
18. Calvert, G.A. (2001). Crossmodal processing in the human brain: insights from functional neuroimaging studies. Cereb. Cortex *11*, 1110–1123.
19. Macaluso, E., and Driver, J. (2005). Multisensory spatial interactions: a window onto functional integration in the human brain. Trends Neurosci. *28*, 264–271.
20. Giard, M.H., and Peronnet, F. (1999). Auditory-visual integration during multimodal object recognition in humans: a behavioral and electrophysiological study. J. Cogn. Neurosci. *11*, 473–490.
21. Beauchamp, M.S., Argall, B.D., Bodurka, J., Duyn, J.H., and Martin, A. (2004). Unraveling multisensory integration: patchy organization within human STS multisensory cortex. Nat. Neurosci. *7*, 1190–1192.
22. Beauchamp, M.S., Lee, K.E., Argall, B.D., and Martin, A. (2004). Integration of auditory and visual information about objects in superior temporal sulcus. Neuron *41*, 809–823.
23. Ghazanfar, A.A., and Schroeder, C.E. (2006). Is neocortex essentially multisensory? Trends Cogn. Sci. *10*, 278–285.
24. Schroeder, C.E., and Foxe, J. (2005). Multisensory contributions to low-level, 'unisensory' processing. Curr. Opin. Neurobiol. *15*, 454–458.
25. Brosch, M., Selezneva, E., and Scheich, H. (2005). Nonauditory events of a behavioral procedure activate auditory cortex of highly trained monkeys. J. Neurosci. *25*, 6797–6806.
26. Welch, R.B., and Warren, D.H. (1986). Intersensory interactions. In Handbook of Perception and Human Performance, L. Kaufman, K.R. Boff, and J.P. Thomas, eds. (New York: Wiley), pp. 25.1–25.36.
27. Alais, D., and Burr, D. (2004). The ventriloquist effect results from near-optimal bimodal integration. Curr. Biol. *14*, 257–262.
28. Kayser, C., Petkov, C.I., Augath, M., and Logothetis, N.K. (2007). Functional imaging reveals visual modulation of specific fields in auditory cortex. J. Neurosci. *27*, 1824–1835.
29. Lehmann, C., Herdener, M., Esposito, F., Hubl, D., di Salle, F., Scheffler, K., Bach, D.R., Federspiel, A., Kretz, R., Dierks, T., and Seifritz, E. (2006). Differential patterns of multisensory interactions in core and belt areas of human auditory cortex. Neuroimage *31*, 294–300.
30. Schroeder, C.E., and Foxe, J.J. (2002). The timing and laminar profile of converging inputs to multisensory areas of the macaque neocortex. Brain Res. Cogn. Brain Res. *14*, 187–198.
31. Fu, K.M., Johnston, T.A., Shah, A.S., Arnold, L., Smiley, J., Hackett, T.A., Garraghty, P.E., and Schroeder, C.E. (2003). Auditory

Please cite this article in press as: Bonath et al., Neural Basis of the Ventriloquist Illusion, Current Biology (2007), doi:10.1016/j.cub.2007.08.050

cortical neurons respond to somatosensory stimulation. J. Neurosci. *23*, 7510–7515.
32. Warren, J.D., and Griffiths, T.D. (2003). Distinct mechanisms for processing spatial sequences and pitch sequences in the human auditory brain. J. Neurosci. *23*, 5799–5804.
33. Baumgart, F., Gaschler-Markefski, B., Woldorff, M.G., Heinze, H.J., and Scheich, H. (1999). A movement-sensitive area in auditory cortex. Nature *400*, 724–726.
34. Warren, J.D., Zielinski, B.A., Green, G.G., Rauschecker, J.P., and Griffiths, T.D. (2002). Perception of sound-source motion by the human brain. Neuron *34*, 139–148.
35. DiRusso, F., Martinez, A., Sereno, M., Pitzalis, S., and Hillyard, S.A. (2001). The cortical sources of the early components of the visual evoked potential. Hum. Brain Mapp. *15*, 95–111.
36. Tardif, E., Murray, M.M., Meylan, R., Spierer, L., and Clarke, S. (2006). The spatio-temporal brain dynamics of processing and integrating sound localization cues in humans. Brain Res. *1092*, 161–176.
37. Mesulam, M.M. (1999). Spatial attention and neglect: parietal, frontal and cingulate contributions to the mental representation and attentional targeting of salient extrapersonal events. Philos. Trans. R. Soc. Lond. B Biol. Sci. *354*, 1325–1346.
38. Posner, M.I. (1995). Attention in cognitive neuroscience: an overview. In Handbook of Cognitive Neuroscience, M. Gazzaniga, ed. (Cambridge, MA: MIT Press), pp. 615–624.
39. Bertelson, P., Vroomen, J., de Gelder, B., and Driver, J. (2000). The ventriloquist effect does not depend on the direction of deliberate visual attention. Percept. Psychophys. *62*, 321–332.
40. Vroomen, J., Bertelson, P., and de Gelder, B. (2001). The ventriloquist effect does not depend on the direction of automatic visual attention. Percept. Psychophys. *63*, 651–659.
41. Choe, C.S., Welch, R.B., Gilford, R.M., and Juola, J.F. (1975). The "ventriloquist effect": visual dominance or response bias? Percept. Psychophys. *18*, 55–60.
42. Bertelson, P., and Aschersleben, G. (1998). Automatic visual bias of auditory location. Psychon. Bull. Rev. *5*, 482–489.
43. Recanzone, G.H. (1998). Rapidly induced auditory plasticity: the ventriloquism aftereffect. Proc. Natl. Acad. Sci. USA *95*, 869–875.
44. Talairach, J., and Tournoux, P. (1988). Co-Planar Stereotaxic Atlas of the Human Brain (New York: Tieme).
45. Kanowski, M., Rieger, J.W., Noesselt, T., Tempelmann, C., and Hinrichs, H. (2007). Endoscopic eye tracking system for fMRI. J. Neurosci. Methods *160*, 10–15.
46. Beauchamp, M.S. (2005). Statistical criteria in FMRI studies of multisensory integration. Neuroinformatics *3*, 93–113.